

stability can be stabilized by the applied magnetic field only. Beam-transverse-temperature stabilization, according to the Bennett pinch condition, Eq. (12), does not occur because of a finite resistivity in the background plasma. In present experimental regimes, the mode is of the resistive type.

I would like to thank Gregory Benford, C. W. Roberson, and Norman Rostoker for many useful discussions.

---

\*Work supported in part by U. S. Energy Research and Development Administration Contracts No. AT(04-3)34 PA207 (University of California, Irvine) and No. EA(11-1)-3070 (Massachusetts Institute of Technology).

<sup>1</sup>G. Yonas and P. Spence, Physics International Co. Report No. PIFR-106, 1968 (unpublished).

<sup>2</sup>P. W. Spence, B. Ecker, and G. Yonas, Bull. Am. Phys. Soc. 14, 1007 (1969).

<sup>3</sup>C. Stallings, Physics International Co. Report No. PIFR-366, 1972 (unpublished).

<sup>4</sup>C. A. Kapetanacos, Appl. Phys. Lett. 25, 484 (1974).

<sup>5</sup>E. S. Weibel, Phys. Rev. Lett. 2, 83 (1959).

<sup>6</sup>H. P. Furth, Phys. Fluids 6, 48 (1963).

<sup>7</sup>S. Hamasaki, Phys. Fluids 11, 1173, 2724 (1968).

<sup>8</sup>M. Bornatici and K. F. Lee, Phys. Fluids 13, 3007 (1970).

<sup>9</sup>K. F. Lee and J. C. Armstrong, Phys. Rev. A 4, 2087 (1971).

<sup>10</sup>G. Benford, Phys. Rev. Lett. 28, 1242 (1972), and Plasma Phys. 15, 483 (1973).

<sup>11</sup>R. Lee and M. Lampe, Phys. Rev. Lett. 31, 1390 (1973).

<sup>12</sup>W. H. Bennett, Phys. Rev. 45, 890 (1934).

<sup>13</sup>D. Prono, B. Ecker, N. Bergstrom, J. Benford, and S. Putnam, Physics International Co. Report No. PIFR-557, 1975 (unpublished).

---

## Impurity Transport in a Quiescent Tokamak Plasma\*

S. A. Cohen, J. L. Cecchi, and E. S. Marmor

*Plasma Physics Laboratory, Princeton University, Princeton, New Jersey 08540*

(Received 14 July 1975)

We have injected short bursts of aluminum into the adiabatic-toroidal-compressor (ATC) tokamak, and measured the time evolution of the radial distribution of highly ionized states of aluminum. The results are compared with a computer code describing neoclassical impurity diffusion.

The transport of high- $Z$  ions in tokamak plasmas is of crucial importance because impurity profiles greatly affect radiation losses,<sup>1</sup> reactivity,<sup>2</sup> and stability,<sup>3</sup> as well as the efficacy of the various heating schemes.<sup>4</sup> Considerable efforts have been made to measure intrinsic impurity content<sup>5,6</sup> and profiles.<sup>7,8</sup> However, it is difficult to determine transport coefficients from these experiments because of the lack of knowledge of the impurity source function. By employing a new impurity injection technique<sup>9</sup> in conjunction with vacuum ultraviolet (VUV) spectroscopy, we have been able to measure the radial transport of aluminum ions in a dirty ( $Z_{\text{eff}}=4.6$ ),<sup>10</sup> quiescent (no large kinklike modes), tokamak plasma. The measurements have been compared with a computer code describing Pfirsch-Schlüter impurity diffusion<sup>11</sup> and agreement is found. We consider this to be further evidence of the neoclassical behavior of ions in tokamaks.

The details of the impurity injection technique have been described elsewhere.<sup>9</sup> High-power laser irradiation of an aluminized glass slide

produces a 300- $\mu$ sec burst containing  $\sim 5 \times 10^{16}$  neutral aluminum atoms with  $\sim 3$  eV mean energy. These atoms are directed into the adiabatic-toroidal-compressor (ATC) tokamak, in which the total number of electrons is approximately  $10^{19}$ . The injected aluminum atoms penetrate about 2 cm into the plasma before being ionized to AlII. The ionization process continues as the ions rapidly circulate along the field lines and, less rapidly, move across them. The time evolution of the line integral of the emissivity for different aluminum ionization states is measured using an absolutely calibrated, grazing-incidence VUV monochromator (McPherson Model No. 247). Observations are made of the strong  $\Delta n=0$  transitions to the ground state ( $\lambda=278.7, 309.6, 352.2, 388.0, 385.0, 332.8, \text{ and } 550.01 \text{ \AA}$  for Al V, VI, VII, VIII, IX, X, and XI, respectively).

During these experiments magnetic probes showed that no large magnetohydrodynamic kinklike modes were present and that the up-down and in-out stability was  $\pm 1.0$  cm. With use of a 4-mm microwave interferometer the average

electron density,  $\langle n_e \rangle$ , was measured. Within 4 msec after aluminum injection  $\langle n_e \rangle$  increased 5% above the no-injection case. The 5% increase is consistent with the amount of aluminum injected. This change in  $\langle n_e \rangle$  decayed with a 7-msec time constant. However, Thomson-scattering measurements of the electron temperature and density profiles showed no discernible changes, i.e.,  $\Delta T_e/T_e, \Delta n_e/n_e \leq 0.1$ ; hence it was not possible to determine if the increase or the decay of  $\langle n_e \rangle$  was due to either a change in the total number of electrons or a change in the  $n_e$  profile. The peak electron density and temperature were  $2.5 \times 10^{13} \text{ cm}^{-3}$  and 1400 eV, respectively; the electron density radial profile is approximately parabolic. The safety factor,  $g(r)$ ,<sup>12</sup> computed from the Thomson-scattering data,<sup>13</sup> was 0.6, 1.0, and 3.0 at  $r=0, 7,$  and 17 cm, respectively.  $Z_{\text{eff}}$ , also computed from the Thomson-scattering data, was 4.6. Most of this is accounted for by the measured oxygen concentration in the plasma. However, measurement of the radial distribution of the total oxygen density is not possible by UV techniques because most of it is fully stripped. The peak proton temperature was approximately 180 eV. Profiles of proton temperature and density have not been measured in ATC; however, measurements on the ST<sup>14</sup> and ORMAK<sup>15</sup> tokamaks, as well as computer simulations<sup>16</sup> for ATC, show nearly parabolic proton temperature and density profiles.

After injection, observations of different Al ionization states were made along chords of the minor cross section. These were Abel inverted<sup>17</sup> and the impurity density was unfolded from

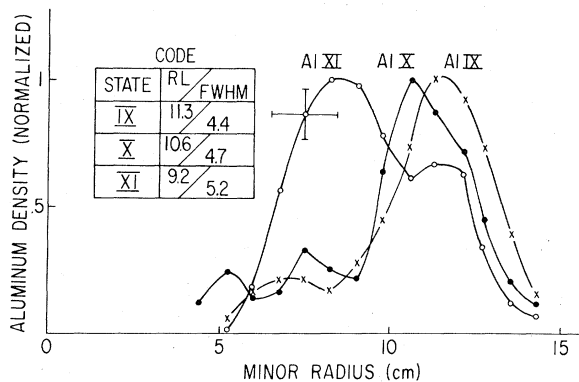


FIG. 1. Radial distributions of Al IX, X, and XI measured at the time of their peak intensity. The inset shows the calculated radial positions (RL) and full widths at half-maxima (FWHM) for the same states.

the photon signals. The salient feature of the results is that each ionization state appears in a particular cylindrical shell of the plasma. The density of a particular ionization state increases in time, then decreases, but does not discernibly move from its shell. The normalized radial distributions of three adjacent ionization states, Al IX, X, and XI, are shown in Fig. 1. The time evolution of the normalized line integral (across the minor diameter) of photon signals from five consecutive ionization states is shown in Fig. 2(a). The  $t=0$  point represents the time at which the aluminum neutrals entered the plasma. These three measurements—the radial profiles, the time evolutions, and the peak absolute brightnesses [Fig. 3(a)]—form a complete description of aluminum transport in the region 8 to 14 cm.

To compare these results with theory we have developed a one-dimensional computer code that describes impurity diffusion in the Pfirsch-Schlüter regime. This code numerically integrates the following set of coupled equations,

$$\frac{\partial n_j}{\partial t} = -\frac{1}{r} \frac{\partial r \Gamma_j}{\partial r} + S_j, \quad j = 1, \dots, 13, \quad (1)$$

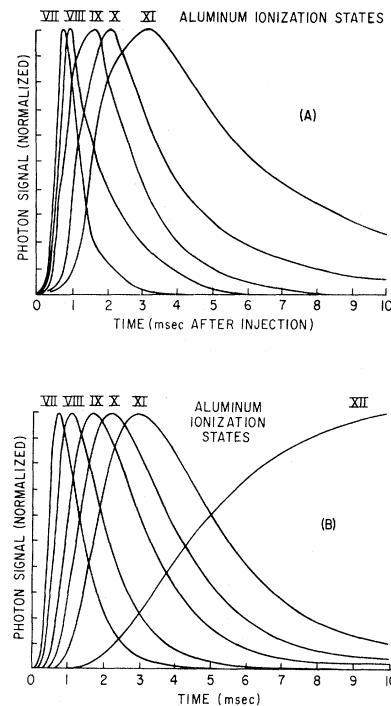


FIG. 2. Time evolution of the normalized line integral of Al photon signals. (a) Experimental; (b) calculated.

with the flux of the  $j$ th ionization state given by<sup>18</sup>

$$\Gamma_j = \sum_b \frac{\rho_b Z_b^2 \nu_{bj}}{Z_j T_b} (1 + \alpha_1 q^2) \left( T_b \frac{\partial n_b}{\partial r} - \frac{n_b Z_b}{n_j Z_j} T_j \frac{\partial n_j}{\partial r} \right), \quad (2)$$

where

$$\nu_{bj} = 4(2\pi)^{1/2} n_j Z_j^2 Z_b^2 e^4 \ln \Lambda / 3m_{ab}^{1/2} T_b^{3/2};$$

$n_b$ ,  $m_{ab}$ ,  $T_b$ ,  $Z_b$ , and  $\rho_b$  are the density, reduced mass, temperature, charge state, and Larmor radius of the background ions ( $b = \text{oxygen}$  and  $\text{hydrogen}$ );  $n_j$  is the density of the  $j$ th ionization state of aluminum, e.g.,  $j = 5$  for Al VI; and  $S_j$  is the sum of source terms of the  $j$ th ionization state. These include electron impact ionization,<sup>19</sup> dielectronic,<sup>20</sup> and radiative<sup>21</sup> recombination.  $\alpha_1$  is a constant of order unity.<sup>18</sup>

We have calculated that diffusion caused by collisions between different Al ionization states, as well as temperature-gradient contributions, is negligible. In the code we specify that there is no recycling of Al lost at the edge. The different ion species are assumed to have temperatures equal to the proton temperature. The electron and proton density profiles are assumed to be stationary in time and to have equal logarithmic spatial derivatives given by the measured electron profile. The absolute concentration of oxygen is set so that  $Z_{\text{eff}} = 4.6$  on axis. The oxygen ionization states are determined from the steady-

state corona model<sup>22</sup> in the region  $r = 0$  to 14 cm. Outside this volume the oxygen is assumed to be ionized five times. The initial distribution of Al II was calculated from the measured energy distribution of the injected neutrals<sup>9</sup> and the measured electron temperature and density profiles of ATC.

Both the spread of velocity and the drift distance of the injected aluminum from the slide to the torus were taken into account in the computer-code source function. However, the spreading in time of the particles along the field lines to the azimuthal position of the monochromator was not included since the interval is smaller than the experimental uncertainties.

The results of the code are in good agreement with the experiment. The code does predict the "stationary shell" effect. The inset in Fig. 1 shows the code predictions for the radial location and the width of the radial distribution of Al IX, X, and XI. Figures 2(b) and 3(b) show the predicted time evolution and absolute brightness<sup>21</sup> for the observed line of each state. In all, only the brightness of Al XI does not give good agreement.

The uncertainties in comparing the code with the experiment must be stressed. The diffusional flux of aluminum due to collisions with oxygen ions is comparable to that due to collisions with the protons, and the oxygen profile is the least accurately known quantity. However, if the oxygen gradient is any steeper than we have assumed, the diffusion must be slower than neoclassical. We have also investigated the effects on the code of varying the proton and electron temperatures. Taking into account all the aforementioned uncertainties and uncertainties in the source-term rates, we infer that the diffusion coefficient is equal to the theoretical one [see Eq. (1)] with an uncertainty of a factor of 3.

Groups at the ORMAK,<sup>23</sup> T-4,<sup>24</sup> and ATC<sup>16</sup> tokamaks have investigated ion thermal conductivity and found it to be neoclassical. Groups at the T-3<sup>7</sup> and ATC<sup>8</sup> tokamaks have investigated impurity transport and conclude that it is inward. The present work also reports inward diffusion with a transport coefficient close to neoclassical.

However, x-ray experiments on the ST<sup>25</sup> tokamak have shown no peaking of the impurity profile on

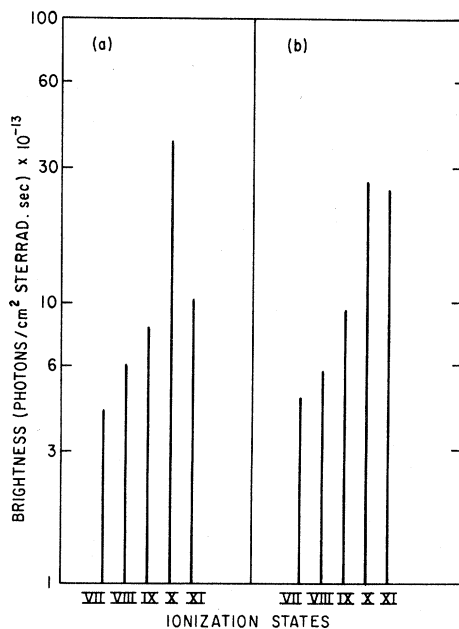


FIG. 3. Absolute peak brightness of Al lines. (a) Experimental; (b) calculated.

axis. We stress that our transport studies were performed in the region outside the  $g = 1$  surface. It is possible that transport inside this region is turbulent and hence peaking of the impurity profile is avoided.

We wish to thank H. P. Furth, R. J. Goldston, E. Mazzucato, and P. H. Rutherford for useful discussions; C. C. Daughney for providing the Thomson-scattering data; and R. Schoemaker and R. Moore for their able technical assistance.

\*Work supported by U. S. Energy Research and Development Administration Contract No. AT(11-1)-3073.

<sup>1</sup>D. M. Meade, Nucl. Fusion 14, 289 (1974).

<sup>2</sup>D. L. Jassby, private communications.

<sup>3</sup>D. W. Ross, Nucl. Fusion 14, 447 (1974).

<sup>4</sup>J. P. Girard, D. Marty, and P. Moriette, in *Proceedings of the Fifth International Conference on Plasma Physics and Controlled Thermonuclear Fusion Research, Tokyo, Japan, 1974* (International Atomic Energy Agency, Vienna, Austria, 1975), Paper No. A17-2.

<sup>5</sup>N. Bretz *et al.*, in *Proceedings of the Fifth International Conference on Plasma Physics and Controlled Thermonuclear Fusion Research, Tokyo, Japan, 1974* (International Atomic Energy Agency, Vienna, Austria, 1975), Paper No. A3-1.

<sup>6</sup>F. Demarco, Plasma Physics Laboratory, Princeton University, Report No. MATT-1012, 1973 (unpublished).

<sup>7</sup>V. I. Gervids and V. A. Krupin, Pis'ma Zh. Eksp. Teor. Fiz. 18, 106 (1973) [JETP Lett. 18, 60 (1973)].

<sup>8</sup>J. L. Cecchi, Bull. Am. Phys. Soc. 19, 853 (1974).

<sup>9</sup>E. S. Marmar, J. L. Cecchi, and S. A. Cohen, Rev. Sci. Instrum. 46, 1149 (1975).

<sup>10</sup> $Z_{\text{eff}} \equiv (\sum Z_i^2 n_i) / (\sum Z_i n_i)$ , where  $n_i$  is the density of the  $i$ th ion species with charge  $Z_i$ .

<sup>11</sup>P. H. Rutherford, Phys. Fluids 17, 1893 (1974).

<sup>12</sup> $q(r) \equiv B_T r / B_p R$ , where  $B_T$  and  $B_p$  are the toroidal

and poloidal magnetic fields, respectively, and  $r$  and  $R$  are the minor and major plasma radii, respectively.

<sup>13</sup>C. C. Daughney, Nucl. Fusion (to be published).

<sup>14</sup>D. Dimock *et al.*, in *Proceedings of the Fourth International Conference on Plasma Physics and Controlled Nuclear Fusion Research, Madison, Wisconsin, 1971* (International Atomic Energy Agency, Vienna, Austria, 1972), Vol. 1, p. 451.

<sup>15</sup>J. Lyon, private communications.

<sup>16</sup>P. H. Rutherford, private communications; P. E. Stott *et al.*, Nucl. Fusion 15, 431 (1975).

<sup>17</sup>W. Lochte-Holtgreven, in *Plasma Diagnostics*, edited by W. Lochte-Holtgreven (North-Holland, Amsterdam, 1968).

<sup>18</sup>We extend the results of Ref. 11 to the case of the aluminum diffusing in a background plasma containing two species of ions. It is assumed that the amount of Al injected is small enough to ignore changes in the proton and oxygen gradients caused thereby, and that three-body collisions can be neglected. The diffusion is calculated in each background species separately, and the results are added linearly.

<sup>19</sup>W. Lotz, Astrophys. J. Suppl. Ser. 14, 207 (1967).

<sup>20</sup>W. Huebner, A. Merts, and B. Cowan, private communication.

<sup>21</sup>Both radiative-recombination and electron-impact-excitation rates are taken from R. C. Elton, in *Methods of Experimental Physics*, edited by H. R. Griem and R. H. Lovberg (Academic, New York, 1970), Vol. 9, Pt. A.

<sup>22</sup>R. W. McWhirter, in *Plasma Diagnostic Techniques*, edited by R. H. Huddlestone and S. L. Leonard (Academic, New York, 1965).

<sup>23</sup>L. A. Berry, J. F. Clarke, and J. T. Hogan, Phys. Rev. Lett. 32, 362 (1974).

<sup>24</sup>E. P. Gorbunov, V. S. Zaverjaev, and M. P. Petrov, in *Proceedings of the Sixth European Conference on Controlled Fusion and Plasma Physics, Moscow, U. S. S. R., 1973* (U.S.S.R. Academy of Sciences, Moscow, 1973), Vol. 1, p. 1.

<sup>25</sup>S. von Goeler *et al.*, Nucl. Fusion 15, 301 (1975).